

A Simple Measurement of Turbulence in Cores of Galaxy Clusters

Yutaka Fujita

*National Astronomical Observatory, Osawa 2-21-1, Mitaka, Tokyo 181-8588, Japan, and
Department of Astronomical Science, The Graduate University for Advanced Studies,
Osawa 2-21-1, Mitaka, Tokyo 181-8588, Japan.*

yfujita@th.nao.ac.jp

ABSTRACT

Using a simple model, we study the effects of turbulence on the motion of bubbles produced by AGN jet activities in the core of a galaxy cluster. We focus on the turbulence with scales larger than the size of the bubbles. We show that for a bubble pair with an age of $\sim 10^8$ yr, the projected angle between the two vectors from the cluster center to the two bubbles should be $\gtrsim 90^\circ$ and the ratio of their projected distances from the cluster center should be $\lesssim 2.5$, if the velocity and scale of the turbulence are $\sim 250 \text{ km s}^{-1}$ and $\sim 20 \text{ kpc}$, respectively. The positions of the bubbles observed in the Perseus cluster suggest that the turbulent velocity is $\gtrsim 100 \text{ km s}^{-1}$ for the cluster.

Subject headings: cooling flows — galaxies: clusters: general — galaxies: active — galaxies: clusters — turbulence

1. Introduction

In the central region of a galaxy cluster, the radiative cooling time of intracluster medium (ICM) is generally much smaller than the Hubble time. In the absence of any heating sources, this means that the ICM flows subsonically toward the cluster center with a mass deposition rate of $\dot{M} \sim 100\text{--}1000 M_\odot$ (Fabian 1994). This flow had been known as a ‘cooling flow’. However, *ASCA* and *XMM-Newton* failed to detect emission from low temperature gas, implying that the actual cooling rate is at least 5 or 10 times smaller than that previously assumed (e.g. Ikebe et al. 1997; Makishima et al. 2001; Peterson et al. 2001; Tamura et al. 2001; Kaastra et al. 2001). These observations strongly suggest that the mass deposition must be prevented by some additional source of heat that balances radiative losses.

Turbulence in the ICM may work as a heating source. Through turbulent mixing, it transfers thermal energy from the outer layer of a cluster into the core (Cho et al. 2003;

Kim & Narayan 2003; Voigt & Fabian 2004). Dissipation of the turbulence can also heat the core. The evidence of turbulence has indirectly observed. For example, Churazov et al. (2004) found that there is little evidence of resonant scattering in the Perseus cluster, which suggests motion of the ICM. Recently, Fujita, Matsumoto, & Wada (2004) showed that bulk gas motion induced by cluster mergers and radiative cooling develop turbulence in and around a core. The reason is that the cool and dense core cannot be moved by the bulk gas motion, and the resultant relative gas motion between the core and the surrounding ICM leads to hydrodynamic instabilities. The core is heated by the turbulence. Since the turbulence is produced and the heating is effective only when the core is cooling and dense, fine-tuning of balance between cooling and heating is alleviated for this model. On the other hand, the activities of the active galactic nuclei (AGNs) at cluster centers may also create turbulence. In particular, the bubbles formed through the AGN activities may move outward in the ICM via buoyancy and may create turbulence behind them (Churazov et al. 2001; Quilis, Bower, & Balogh 2001; Saxton, Sutherland, & Bicknell 2001).

These two types of turbulence have different features. The typical scale of the turbulence produced by the bulk gas motion in the ICM is close to the size of a cluster core ($\gtrsim 20$ kpc; Fujita et al. 2004, 2005). This scale is larger than the typical size of a bubble (~ 10 kpc; Fabian et al. 2003). Thus, the bubble, if any, will be staggered in the velocity fields of the turbulence. On the other hand, the maximum scale of the turbulence produced by a buoyant bubble should be limited to the size of the bubble. Since the bubble is the engine of the turbulence, its motion should not be affected much by the turbulence.

Recently, old bubbles have been observed in the X-ray and radio bands. They are located away from cluster centers. In the Virgo cluster, diffuse radio emission from possible old bubbles was observed at a distance of $\gtrsim 20$ kpc from the cluster center (Owen et al. 2000). From X-ray observations, ‘arms’ of cold gas have been found; they might be cold gas entrained by the old bubbles from the cluster center (Churazov et al. 2001; Belsole et al. 2001; Molendi 2002; Young et al. 2002). The arms may indicate the paths of the bubbles. For the Perseus cluster, two bubble pairs (four bubbles) have been found by *Chandra* (Fabian et al. 2002). While the inner pair is at $r \sim 5$ kpc from the cluster center, the outer pair is at $r \sim 40$ kpc.

If a bubble pair is formed through AGN jet activities, the initial positions of the two bubbles are expected to be symmetric about the cluster center, where the AGN is located. There are several clusters for which high-resolution X-ray and radio observations were made and the positions of newborn twin bubbles were obtained. Among such clusters, Hydra A, A2052, M84, Cygnus A, and Centaurus respectively have two bubbles that are next to the central AGNs and the positions are consistent with being symmetric about the AGNs

(McNamara et al. 2000; Blanton et al. 2001; Finoguenov & Jones 2001; Smith et al. 2002; Fabian et al. 2005). On the other hand, the positions of the two inner bubbles in the Perseus cluster do not appear to be symmetric about the AGN (the upper panel of Fig. 1 in Fabian et al. 2002). However, radio observations showed that the directions of jets are symmetric and a new bubble pair appears to be forming in those directions (the upper panel of Fig. 3 in Fabian et al. 2002). The complicated shapes of the inner bubbles may be due to the projection of a few bubble pairs.

In contrast with the newborn bubbles, the positions of the old bubbles are not always symmetric about the cluster centers. For the Virgo cluster, the angle between the two arms is $\sim 135^\circ$ (Figure 1 [upper right] of Churazov et al. 2001). Moreover, the arms are not straight and they are bent at $r \sim 20$ kpc (Forman et al. 2005). For the Perseus cluster, although no clear arms have been observed, the angle between the two vectors from the cluster center to the two outer old bubbles is $\sim 120^\circ$. In this letter, we study how the large-scale turbulence, which is not created by bubble motions, affects the motion of the bubbles and makes the observed asymmetries. We use the Hubble constant of $H_0 = 70 \text{ km s}^{-1} \text{ Mpc}^{-1}$.

2. Models

We assume that the gravitational potential of a cluster is spherically symmetric and the central AGN creates two spherical bubbles near the cluster center. At $t = 0$, the bubbles are at a radius R_0 from the cluster center in the opposite directions with respect to the cluster center. Each bubble moves outward in the cluster via buoyancy. The equation of motion for a bubble is

$$m_{\text{bub}} \frac{d\mathbf{u}}{dt} = m_{\text{bub}} \mathbf{g} - \rho |\mathbf{u} - \mathbf{u}_t| (\mathbf{u} - \mathbf{u}_t) \pi r_{\text{bub}}^2 - \frac{4}{3} \pi r_{\text{bub}}^3 \nabla P, \quad (1)$$

where m_{bub} is the mass of the bubble, \mathbf{u} is the velocity of the bubble, \mathbf{u}_t is the velocity of turbulence at the position of the bubble, \mathbf{g} is the gravitational acceleration, r_{bub} is the radius of the bubble, and P is the ICM pressure at the position of the bubble. We assume that a bubble is adiabatic and in pressure equilibrium with the surrounding ICM. Thus, the radius of the bubble has the relation of

$$r_{\text{bub}} = r_{\text{bub},0} (P/P_0)^{1/3\gamma}, \quad (2)$$

where $r_{\text{bub},0}$ is the initial radius of the bubble, P_0 is the ICM pressure at the position where the bubble is created, and γ ($= 4/3$) is the adiabatic constant.

For the sake of simplicity, we assume that the turbulence has a monochromatic spectrum with a velocity of u_t and a spatial scale of l_t . We divide a cluster into small cubes with a

side of l_t . We assume that in each cube, the velocity field of the ICM is uniform, that is, the velocity and the direction are constant. The direction has no correlation among the cubes.

For parameters of a model cluster, we use the results of *XMM-Newton* observations of the Perseus cluster. We chose the cluster because there were a few studies about turbulence in the cluster (Churazov et al. 2004; Rebusco et al. 2005). Churazov et al. (2003) obtained the density and temperature profiles of the cluster (their equations [4] and [5]). We assume that the ICM is in pressure equilibrium, because the velocity of the turbulence is smaller than the sound velocity of the ICM. From the density and temperature profiles, ignoring the self-gravity of the ICM, we derived the mass profile of the cluster, $M(R)$, where R is the distance from the cluster center.

3. Results and Discussion

We assume that the initial radii of bubbles are $r_{\text{bub},0} = 10$ kpc and their initial positions are $R_0 = 10$ kpc. The bubble mass, m_{bub} , is 0.01 times the mass of the ambient gas with the same volume. The results are not sensitive to m_{bub} , as long as it is small. We calculated the motion of bubbles for several kinds of turbulence. Since $r_{\text{bub}} \sim 10$ kpc, we limited l_t to be ≥ 10 kpc. The model parameters are shown in Table 1. They are based on the results of numerical simulations of a cluster core (Fujita, Matsumoto, & Wada 2004; Fujita et al. 2005). Other studies also suggested the existence of similar velocity fields in cluster cores. Dennis & Chandran (2005) studied the balance between turbulent heating and radiative cooling in clusters. Comparing their model with observations, they concluded that $100 \lesssim u_t \lesssim 300 \text{ km s}^{-1}$ if $l_t = \alpha R + l_0$, where $0.05 < \alpha < 1$ and $l_0 = 0.5$ kpc. Rebusco et al. (2005) also obtained the values similar to those shown in Table 1 from the observed metal distribution in the core of the Perseus cluster. Note that while the method invented by Rebusco et al. (2005) measures the velocity fields averaged on a time-scale of \gtrsim Gyr (the time-scale of metal ejection from stars), our method measures those averaged on a time-scale of ~ 0.1 Gyr (the age of bubbles; see below).

Since the expansion velocity of a bubble at the formation is larger than u_t in Table 1 (e.g. Soker, Blanton, & Sarazin 2002), we assume that the initial velocity of the bubbles is $u = 0$. For each turbulence model, we randomly chose the initial direction of the line connecting the two bubbles, the position of the cluster center in the cube that contains the cluster center, and the viewing angle; they are independent each other. For each model, we calculated the motions of 10,000 bubble pairs and their projected positions at $t = 10^8$ yr.

Figure 1 shows the projected trajectories of five randomly selected bubble pairs for

$l_t = 20$ kpc and $u_t = 250$ km s⁻¹ (Model A2). The end points correspond to $t = 10^8$ yr. We found that the bubbles reach projected distances of $b \sim 10$ –50 kpc from the cluster center, which are similar to the positions of the outer bubbles observed in the Perseus cluster (33 and 38 kpc). Although there are exceptions, the bubbles move fairly straight from their departure points (at least not zigzag), because u_t is smaller than the velocity driven by buoyancy alone (~ 440 km s⁻¹). This is almost the same for other models except for model B2 ($u_t = 500$ km s⁻¹).

Figure 2 shows the distributions of the projected angle θ between the two vectors from the cluster center to the two bubbles composing a pair. If the two bubbles are located in the opposite directions with respect to the cluster center, $\theta = 180^\circ$. In model A2, for example, about 90% of bubble pairs have $\theta \gtrsim 90^\circ$. The angle θ has a wider distribution for larger u_t and l_t because the bubbles are scattered more effectively by the turbulence. This scatter works as diffusion in the θ -space. Medians of the angle are $\theta_m \sim 120$ –150° except for model B1 (Table 1). In model B1, almost all bubble pairs have $\theta \approx 180^\circ$, because u_t is much smaller than the velocity driven by buoyancy. In model B2, there is no preferential angle (Figure 2b). For the Perseus cluster, the angle between the two outer bubbles is $\theta = 120^\circ$. In Table 1, we show the fraction of bubble pairs with $\theta > 120^\circ$. The values of $f(\theta > 120^\circ)$ indicate that the angle distributions of all the models except for model B1 are consistent with the observation. In model B1, the value of θ for the Perseus cluster is unacceptably small (the probability is <1%), which means that u_t is too small to account for the observation. For the cluster, $u_t \gtrsim 100$ km s⁻¹ is required, which could be detected by *SUZAKU*.

We refer to b_i ($i = 1, 2$) as the projected distances of the two bubbles composing a pair from the cluster center. Figure 3 shows the distributions of the ratio $\Gamma = \max(b_1/b_2, b_2/b_1)$. In model A2, for example, about 90% of bubble pairs have $\Gamma \lesssim 2.5$. As is the case of θ , the ratio has a wider distribution for larger u_t and l_t . Medians of the ratio, Γ_m , are also shown in Table 1. For the two outer bubbles in the Perseus cluster, the ratio is 1.15, and the fractions of bubble pairs with a ratio larger than this, $f_\Gamma(> 1.15)$, are shown in Table 1. All models are consistent with the observation, although model B1 is less preferable. We also studied the two dimensional distributions of θ and Γ . We found no strong correlation between them.

Since the effective diffusion coefficient for the bubble motion is represented by $D \propto u_t l_t$, models A3 and B2 have the same coefficient. However, the angle and ratio distributions of the two models are different (Figures 2 and 3); those of model A3 have narrower distributions. This is because for model A3 the turbulent velocity, u_t , is much smaller than the buoyant velocity, and thus the final positions of the bubbles are mainly determined by buoyancy. In the future, with more observations about the positions of old bubbles in clusters, we could more tightly constrain the typical velocity and scale of turbulence in cluster cores.

We note that the systematic motion of the cD galaxy containing an AGN with respect to the ICM, v_p , may affect the asymmetry of bubble positions. On the frame that moves with the cD galaxy, this can be studied as the case of $l_t = \infty$ and $u_t = v_p$. Our results may indicate that $v_p \gtrsim 100 \text{ km s}^{-1}$ for the Perseus cluster, and this could be observed by *SUZAKU* as the shift of metal lines from the optical redshift of the cD galaxy. Since the observed bubbles are inside the potential wells of cD galaxies, the aspherical potential of a cD galaxy could also affect of the asymmetry of bubble positions. The former could be measured from the optical image of the galaxy. For the Perseus cluster, the ratio of the major axis to the minor axis in a red color is < 1.1 ,¹ which does not affect the results above.

4. Conclusions

Using a simple model, we have investigated the turbulence at scales larger than the size of bubbles observed in cool cores of galaxy clusters. We showed that for a bubble pair, which was created by AGN jet activities $\sim 10^8$ yrs ago, the projected angle between the two vectors from the cluster center to the two bubbles should be $\gtrsim 90^\circ$, and the ratio of their projected distances from the cluster center should be $\lesssim 2.5$, if the velocity and scale of turbulence are $\sim 250 \text{ km s}^{-1}$ and $\sim 20 \text{ kpc}$, respectively. The positions of the bubbles observed in the Perseus cluster indicate that the velocity is $\gtrsim 100 \text{ km s}^{-1}$ for the cluster. This turbulence could directly be detected by *SUZAKU*. Fabian et al. (2003) indicated that the ICM is not turbulent at the scale of $\lesssim 10 \text{ kpc}$. Detailed observations of X-ray spectra may reveal the lower limit of the scale of turbulence (Inogamov & Sunyaev 2003), which might be determined by the viscosity of the ICM (Schuecker et al. 2004).

I thank the anonymous referee for useful comments. Y. F. was supported in part by a Grant-in-Aid from the Ministry of Education, Culture, Sports, Science, and Technology of Japan (17740182).

REFERENCES

- Belsole, E., et al. 2001, *A&A*, 365, L188
- Blanton, E. L., Sarazin, C. L., McNamara, B. R., & Wise, M. W. 2001, *ApJ*, 558, L15

¹NED: <http://nedwww.ipac.caltech.edu/>

- Cho, J., Lazarian, A., Honein, A., Knaepen, B., Kassinos, S., & Moin, P. 2003, *ApJ*, 589, L77
- Churazov, E., Brüggén, M., Kaiser, C. R., Böhringer, H., & Forman, W. 2001, *ApJ*, 554, 261
- Churazov, E., Forman, W., Jones, C., Böhringer, H. 2003, *ApJ*, 590, 225
- Churazov, E., Forman, W., Jones, C., Sunyaev, R., & Böhringer, H. 2004, *MNRAS*, 347, 29
- Dennis, T. J., & Chandran, B. D. G. 2005, *ApJ*, 622, 205
- Fabian, A. C. 1994, *ARA&A*, 32, 277
- Fabian, A. C., Celotti, A., Blundell, K. M., Kassim, N. E., & Perley, R. A. 2002, *MNRAS*, 331, 369
- Fabian, A. C., Sanders, J. S., Allen, S. W., Crawford, C. S., Iwasawa, K., Johnstone, R. M., Schmidt, R. W., & Taylor, G. B. 2003, *MNRAS*, 344, L43
- Fabian, A. C., Sanders, J. S., Taylor, G. B., & Allen, S. W. 2005, *MNRAS*, 360, L20
- Finoguenov, A., & Jones, C. 2001, *ApJ*, 547, L107
- Forman, W. et al. 2005, *ApJ*, in press (astro-ph/0312576)
- Fujita, Y., Matsumoto, T., & Wada, K. 2004, *ApJ*, 612, L9
- Fujita, Y., Matsumoto, T., Wada, K., & Furusho, T. 2005, *ApJ*, 619, L139
- Ikebe, Y. et al. 1997, *ApJ*, 481, 660
- Inogamov, N. A., & Sunyaev, R. A. 2003, *Astronomy Letters*, 29, 791
- Kaastra, J. S., Ferrigno, C., Tamura, T., Paerels, F. B. S., Peterson, J. R., & Mittaz, J. P. D. 2001, *A&A*, 365, L99
- Kim, W. & Narayan, R. 2003, *ApJ*, 596, L139
- Makishima, K. et al. 2001, *PASJ*, 53, 401
- McNamara, B. R., et al. 2000, *ApJ*, 534, L135
- Molendi, S. 2002, *ApJ*, 580, 815
- Owen, F. N., Eilek, J. A., & Kassim, N. E. 2000, *ApJ*, 543, 611

- Peterson, J. R. et al. 2001, *A&A*, 365, L104
- Quilis, V., Bower, R. G., & Balogh, M. L. 2001, *MNRAS*, 328, 1091
- Rebusco, P., Churazov, E., Böhringer, H., & Forman, W. 2005, *MNRAS*, 359, 1041
- Saxton, C. J., Sutherland, R. S., & Bicknell, G. V. 2001, *ApJ*, 563,
- Schuecker, P., Finoguenov, A., Miniati, F., Böhringer, H., & Briel, U. G. 2004, *A&A*, 426, 387
- Smith, D. A., Wilson, A. S., Arnaud, K. A., Terashima, Y., & Young, A. J. 2002, *ApJ*, 565, 195
- Soker, N., Blanton, E. L., & Sarazin, C. L. 2002, *ApJ*, 573, 533
- Tamura, T. et al. 2001, *A&A*, 365, L87
- Voigt, L. M. & Fabian, A. C. 2004, *MNRAS*, 347, 1130
- Young, A. J., Wilson, A. S., & Mundell, C. G. 2002, *ApJ*, 579, 560

Table 1. Model Parameters

Model	l_t (kpc)	u_t (km s ⁻¹)	θ_m (degree)	Γ_m	$f_\theta(> 120^\circ)$	$f_\Gamma(< 1.15)$
A1	10	250	153	1.37	0.82	0.24
A2	20	250	144	1.43	0.72	0.22
A3	40	250	129	1.47	0.58	0.21
B1	20	25	177	1.04	0.998	0.92
B2	20	500	115	1.61	0.47	0.17

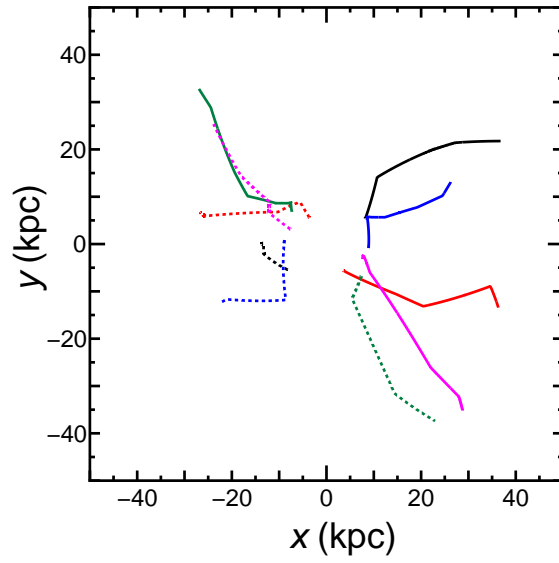


Fig. 1.— Projected trajectories for five randomly selected bubble pairs. A pair is represented by the solid and dotted lines with the same color. The cluster center is $(x, y) = (0, 0)$

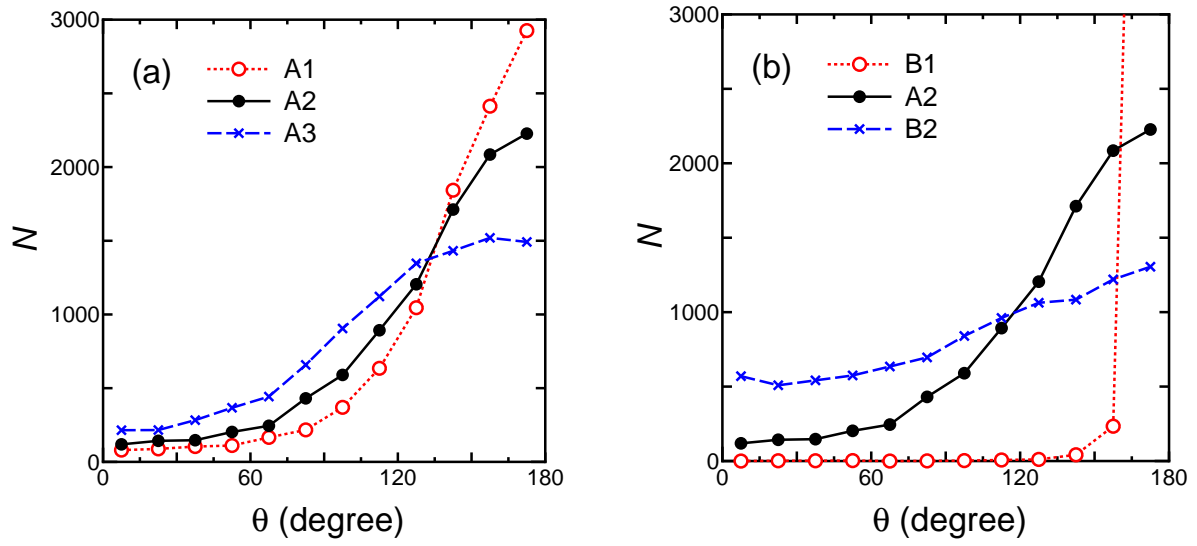


Fig. 2.— (a) Histogram of the angle θ for models A1–A3. (b) Same as (a) but for models B1 and B2.

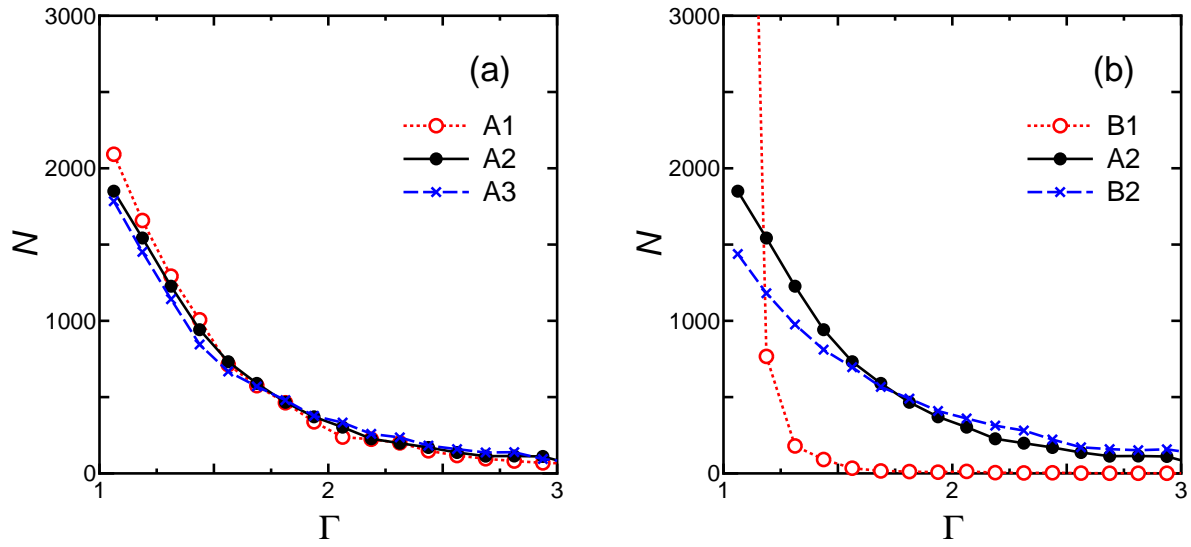


Fig. 3.— (a) Histogram of the ratio Γ for models A1–A3. (b) Same as (a) but for models B1 and B2.